Correspondence

Statistics of the Radio-Frequency Signal Based on K Distribution with Application to Echocardiography

Olivier Bernard, Jan D'hooge, *Member, IEEE*, and Denis Friboulet, *Member, IEEE*

***Abstract*—We study in this paper the statistics of the radio frequency (RF) signal in the case of partially developed speckle. Using the K distribution framework, we give the probability density function of the associated distribution, the corresponding moments, and estimators for the parameters of the distribution. The consistency of the proposed estimators is evaluated in terms of their bias and variance through numerical simulations. The ability of the proposed distribution to model RF echographic signals from cardiac tissues is evaluated from data acquired *in vivo*.**

I. Introduction

Most applications of medical ultrasound imaging are based on the analysis of B-scan images that are constructed from the envelope of the echo signal. In this context, the statistics of the ultrasound echo envelope have been extensively studied for both segmentation [1]–[4] and tissue characterization [5]–[7] purposes. The most commonly used statistical model for the envelope signal is the conventional Rayleigh distribution, which relies on the assumption of a large number of scatterers per resolution cell and corresponds to fully developed speckle [8]. In echocardiography, this model is particularly well suited to characterize reflections from blood, but it fails to model more complex structures such as myocardial tissue. Therefore, K distributions have been proposed to model different kinds of tissue in ultrasound envelope imaging [9]–[11]. The model first has been introduced in the radar domain [12], [13] and has been applied successfully to ultrasound imaging [11] in order to model partially developed speckle, which arises when the scatterers density is small or when the scatterers have varying scattering cross-section.

With the introduction of digital ultrasound devices, the radio-frequency (RF) signal has become more readily available. The interest of such signal resides in the fact that it potentially contains more information than the envelope echo. In practice, this signal is either available as a real signal (usually called simply RF signal) or as a complex signal obtained through demodulation and formally corresponding to the complex envelope of the RF signal (usually called IQ signal for in phase quadrature signal). In contrast, with the statistics of the envelope-detected signal, the statistics of the RF signal in the case of partially developed speckle have not been widely explored in the field of medical ultrasound. Therefore, we propose to describe these statistics and to use them in echocardiography for the modeling of RF signals backscattered from the myocardium. This choice is motivated by the work of Clifford *et al.* [14] who showed that the statistics of the envelope-detected signal backscattered from myocardial regions corresponds to partially developed speckle, and thus can be reliably modeled through a standard K-distribution. In terms of myocardium properties, this phenomenon may be explained either by the clustering of the scatterers in the resolution cell or by a large variability of the scattering cross section, inducing a decrease of the apparent scatterers density [11], [14].

In Section II we briefly recall the theoretical basis for the K distributions and give the probability density function (pdf) of the RF signal and the corresponding moments. In Section III we provide the estimators for the parameters of the distribution. In Section IV, the consistency of the proposed estimators is evaluated in terms of their bias and variance through numerical simulation. In Section V we evaluate the ability of the proposed distribution to model *in vivo* RF data from cardiac images. The main conclusions are given in Section VI.

II. Statistics of the RF Signal Based on the K Distribution

The backscattered ultrasonic signal results from the individual energy contributions of each scatterer embedded in the resolution cell. This situation can be described mathematically as a random walk in the complex plane [8], [11]. From this model, the signal can be expressed as a random process, depending on the number of scatterers present inside the resolution cell, their relative position (structure), and their contribution. This results in a K distribution for the envelope-detected signal when the scatterers position is assumed to be uniformly distributed and when their amplitude is modeled as a K distribution itself [11]–[13]. The pdf of the complex envelope and RF signals given below then can be derived from the pdf of the analytical signal [11] using standard algebraic computation. It is interesting to note that these expressions also can be straightforwardly obtained as a particular case of the multiplicative model designed for the modeling of extremely heterogeneous clutter in the field of SAR [15].

Manuscript received April 2, 2006; accepted April 28, 2006.

O. Bernard and D. Friboulet are with CREATIS UMR CNRS 5515, U 630 INSERM, Institut National des Sciences Appliquées (INSA), Blaise Pascal, 69621 Villeurbanne Cedex, France (e-mail: bernard@creatis.insa-lyon.fr).

J. D'hooge is with Cardiac Imaging Research, Department of Cardiology and Department of Electronic Engineering, Leuven, Belgium.

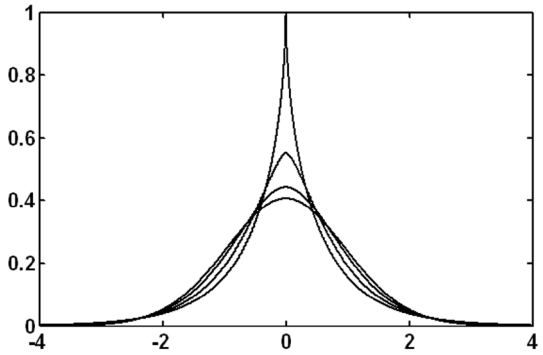

Fig. 1. f_X^{rf} pdf for several values of parameter α: {0.75, 1.5, 4, 20}. The smaller the parameter α value, the sharper the curve. The curves were normalized so that the mean square value of the pdfs is unity.

A. Statistical Expressions for the Radio-Frequency Signal

In this framework, the pdf of the RF signal X is given as:

$$f_X^{\mathrm{rf}}(x) = \frac{b}{\sqrt{\pi}\Gamma(\alpha)} \left(\frac{b\,|x|}{2}\right)^{\alpha-0.5} K_{\alpha-0.5}\left(b\,|x|\right), \quad (1)$$

where Γ is the standard Gamma function and $K_{\alpha-0.5}$ is the modified Bessel function of the second kind of order $\alpha - 0.5$.

The corresponding distribution is called K_{RF} distribution in the remainder of the paper. α and b are, respectively, the shape and scale parameters of the distribution. It is to be noted that the Gaussian distribution is a limiting case of K_{RF} when the parameter α takes on large values. Fig. 1 shows f_X^{rf} for different values of the shape parameter α.

From (1) the moments of the K_{RF} distribution for the absolute value of the random variable may be computed as:

$$\begin{aligned}\mu_n^{\mathrm{rf}} &= E^{\mathrm{rf}}\left[|X|^n\right] \\ &= \frac{1}{\sqrt{\pi}}\left(\frac{2}{b}\right)^n \frac{\Gamma\left((n+1)/2\right).\Gamma\left(\alpha+n/2\right)}{\Gamma(\alpha)}.\end{aligned} \quad (2)$$

B. Statistical Expressions for the Complex Envelope Signal

As mentioned in Section I, the RF signal may be given as a complex envelope, usually called the IQ signal. For completeness, we give the statistics of this representation, which can be derived by following the same scheme as the one used for the RF signal. Let us call $X + jY$ the analytic signal associated to the RF signal. The complex envelope signal $s_e(t) = u + jv$ corresponds to a frequency shift of the analytical signal:

$$u + jv = (X + jY).\exp\left(-j\omega_0 t\right). \quad (3)$$

The resulting complex signal has lower central frequency than the analytic signal, but with the same energy content that makes it very attractive. The joint density function of the real part u and the imaginary part v of the complex envelope signal is obtained as:

$$\begin{aligned}f_{U,V}^{\mathrm{iq}}(u,v) = \frac{1}{2\pi}\frac{2b}{\Gamma(\alpha)}&\left(\frac{b\sqrt{u^2+v^2}}{2}\right)^{\alpha} \\ &\cdot K_{\alpha-1}\left(b\sqrt{u^2+v^2}\right)\frac{1}{\sqrt{u^2+v^2}}.\end{aligned} \quad (4)$$

The corresponding distribution is called K_{IQ} distribution in the remainder of the paper. As in the case of the RF signal, the Gaussian distribution is a limiting case of K_{IQ} distribution corresponding to large values of the shape parameter α. It can be shown from (4) that the moments of the real and imaginary part of the complex signal are the same as the moments of the RF signal as given in (2).

III. Estimation of Parameters

The estimation of the parameters α and b has been thoroughly investigated [16]–[22] for the envelope-detected signal. In this section we give the counterpart of three commonly used estimators for the RF signal.

Because maximum likelihood (ML)-based methods do not lead to a closed form solution in the case of K distribution statistics, most estimators are based on order moments. Using the analytic expression of the K distribution moments, it has been shown [18] that the two parameters of the K distribution can be estimated by using any two estimates of the moments. The simplest approach, called explicit estimator, uses the second- and fourth-order moments. This method has the advantage of being fast and performs well for a large number of samples (> 2000). But it fails when the amount of data is small due to the large variability of the fourth-order moment. In this perspective, an approach based on the first- and second-order moment, called implicit estimator, has been described [21]. This method yields nonlinear equations that have to be solved numerically. Therefore, it is computationally more expensive. Starting from the observation that improved accuracy results when the log of the data is used [16], [17], a new technique was recently proposed by Blacknell [17]. This method is based on the use of log moments to obtain an expression, depending only on the shape parameter that yields an explicit expression for the estimation of α. Using the expression of the moment given in (2), the RF counterpart of these three moment-based estimators for parameter α may be derived as:

Explicit estimator for the RF signal:

$$\frac{E^{\mathrm{rf}}\left[X^4\right]}{E^{\mathrm{rf}}\left[X^2\right]} = 3\left(1 + \frac{1}{\alpha}\right). \quad (5)$$

Implicit estimator for the RF signal:

$$\frac{E^{\mathrm{rf}}\left[X^2\right]}{\left(E^{\mathrm{rf}}\left[|X|\right]\right)^2} = \frac{\pi}{2}\alpha\frac{\Gamma(\alpha)^2}{\Gamma(\alpha+0.5)^2}. \quad (6)$$

TABLE I
ESTIMATED BIAS AND SAMPLE VARIANCE OF α FOR $N = 512$.[1]

	Explicit		Implicit		Blacknell	
α	$E[\hat{\alpha}] - \alpha$	$\mathrm{Var}[\hat{\alpha}]$	$E[\hat{\alpha}] - \alpha$	$\mathrm{Var}[\hat{\alpha}]$	$E[\hat{\alpha}] - \alpha$	$\mathrm{Var}[\hat{\alpha}]$
0.4	0.1485	0.0253	0.0270	0.0032	0.0209	0.0017
0.8	0.2146	0.1110	0.0407	0.0201	0.0385	0.0163
1.2	0.3461	0.4043	0.0919	0.0895	0.0924	0.0850
1.6	0.4507	0.9356	0.1245	0.2157	0.1345	0.2498
2.0	0.7231	2.2788	0.2609	0.6719	0.2955	0.8442

[1]Note, Averages computed over 1000 independent trials in each case.

TABLE II
ESTIMATED BIAS AND SAMPLE VARIANCE OF α FOR $N = 1024$.[1]

	Explicit		Implicit		Blacknell	
α	$E[\hat{\alpha}] - \alpha$	$\mathrm{Var}[\hat{\alpha}]$	$E[\hat{\alpha}] - \alpha$	$\mathrm{Var}[\hat{\alpha}]$	$E[\hat{\alpha}] - \alpha$	$\mathrm{Var}[\hat{\alpha}]$
0.4	0.1224	0.0115	0.0218	0.0018	0.0172	0.0009
0.8	0.1278	0.0510	0.0226	0.0095	0.0226	0.0074
1.2	0.1616	0.1583	0.0311	0.0360	0.0340	0.0328
1.6	0.2580	0.3599	0.0772	0.0998	0.0833	0.1094
2.0	0.2874	0.5905	0.0885	0.1935	0.0973	0.2165

[1]Note, Averages computed over 1000 independent trials in each case

Blacknell estimator for the RF signal:

$$\frac{E^{\mathrm{rf}}\left[X^2 \log|X|\right]}{E^{\mathrm{rf}}\left[X^2\right]} - E^{\mathrm{rf}}\left[\log|X|\right] = 1 + \frac{1}{2\alpha}. \tag{7}$$

Thus, these parameters are obtained from the available data by replacing the various moments in expressions (5), (6), and (7) by their sample version. Once α is estimated, the scale parameter b may be computed from (2) as:

$$b = \sqrt{\frac{2\alpha}{E^{\mathrm{rf}}\left[X^2\right]}}. \tag{8}$$

As the moments expression for the K_{IQ} distribution is the same as the one for the K_{RF} distribution, parameter estimators for the IQ signal also are given by (5), (6), and (7).

IV. Numerical Simulations

In this section, a comparison of the performance of estimators (5)–(7) is presented[1]. Hereto, data distributed according to the pdf given in (1) were generated using the cumulative distribution function (CDF) method [23]. The power of the data was normalized in such a way that the second-order moment of the process was unity by setting:

$$b = \sqrt{2\alpha}. \tag{9}$$

Data were generated for five values of the shape parameter α in the range [0.4, 2.0]. This corresponds to the range observed from the experiments made on different orientations and on different patients, where α was found to vary between 0.4 and 1.2 for myocardial regions. The number of data samples (N) was chosen to be 512 and 1024, respectively. This procedure was followed 1000 times and the corresponding bias and variance are presented in Tables I and II for $N = 512$ and $N = 1024$, respectively. The results show that the bias and variance of the estimators improve as N increases and that they increase with α. The explicit estimator yields the lowest performance. Implicit and Blacknell estimators exhibit lower bias and variance and have similar behavior for small values of α (< 1). The implicit estimator provides slightly better results when α is larger than 1.2. It is interesting to note that these results are in concordance with those obtained from the envelope-based estimator data [19], [21].

[1]As the simulation procedure and the estimators for the RF signal and the real part of the IQ signal are identical, it is noted that the results presented here also hold for the IQ signal.

TABLE III
ORIENTATION OF THE ECHOCARDIOGRAPHIC IMAGES AND LOCATION OF THE PROCESSED TISSUE AREAS.

Orientation	Processed tissue area
Apical 4 chamber (ACH)	Interventricular septum
Apical 2 chamber (A2CH)	Left ventricle anterior wall
Parasternal long axis (PALA)	Left ventricle inferolateral wall
Parasternal short axis (PASA)	Left ventricle inferolateral wall

V. Experimental Results on In Vivo Data

We tested the ability of the distributions defined in Section II to model RF and IQ data on a variety of ultrasound cardiac images of clinical interest. Data were acquired us-

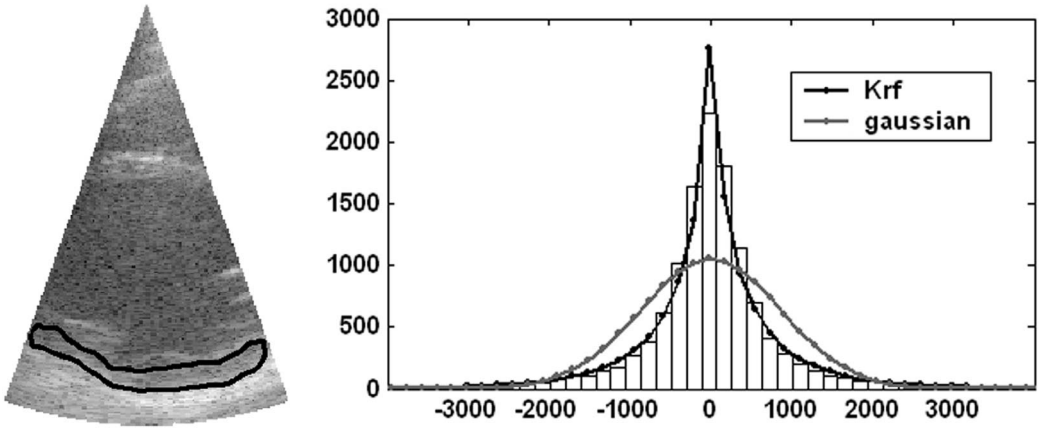

(a) (b)

Fig. 2. Results obtained for a Parasternal long axis view in the myocardial tissue. (a) Parasternal long axis image in which the black curve indicates the myocardium region delimited by a trained cardiologist. (b) Fits of the Gaussian and K_{RF} distributions to the RF data corresponding to the myocardium region shown in (a). For this example, the resulting Freeman-Tuckey measure associated to the K_{RF} and the Gaussian distribution are, respectively, 434 and 4311. The corresponding RMSE is 75 and 192.

TABLE IV
RMSE AND FREEMAN TUCKEY RESULTS FOR RF TISSUE REGIONS.

Orientation	RMSE		Freeman Tuckey measure	
	K_{RF}	Gaussian	K_{RF}	Gaussian
Apical 4 chamber (A4CH)	209	478	1920	14931
Apical 2 chamber (A2CH)	186	289	1830	7547
Parasternal long axis (PALA)	78	147	594	3125
Parasternal short axis (PASA)	344	595	3582	20061

ing a Toshiba Powervision 6000 (Toshiba Medical Systems Europe, Zoetermeer, The Netherlands) equipped with an RF interface for research purposes and a 3.75-MHz probe. The RF signal was acquired without any attenuation correction. The RF sample frequency varied between 25 and 32 MHz according to the acquisition mode. This equipment has the advantage to give access to envelope, RF and IQ signals. Table III summarizes the image views and the left ventricular segments visualized. For each view, five independent RF data sets (from five different, healthy volunteers) were acquired, from which a single image was selected visually to provide easy discrimination between the myocardium region and the blood pool. Subsequently, a trained cardiologist manually drew a contour delimiting a region inside the myocardium. In each region, the fit of the proposed distribution was done for both RF and IQ data. The fit to a Gaussian pdf also was performed and used as a reference for all experiments. The parameter α of the K_{RF} and K_{IQ} pdf was estimated using Blacknell's method.

The ability of the proposed distribution to model the RF data was expressed through the root mean square error (RMSE) and a goodness-of-fit measure. The latter was measured through a Chi-square (χ^2)-type test, which has the interesting property of being able to handle a multivariate pdf such as the K_{IQ} distribution. As the conventional χ^2 test, based on the Pearson's measure [24], is heavily affected by small, expected frequencies that commonly appear when dealing with heavy tail distributions such as experimental RF data, we used the χ^2 Freeman-Tuckey measure instead [24]. The number of bins used to build the histograms from the data was selected according to the approach proposed by D'Agostino and Stephens [25] by setting $M = 2n^{2/5}$, where M is the number of bins and n is the sample size.

In Fig. 2, an example of the fit obtained for a parasternal long axis view in the myocardial tissue, along with the associated Freeman-Tuckey measure and RMSE value, is given. This example illustrates qualitatively how the K_{RF} distribution better fits the data than the Gaussian. This corresponds quantitatively to a lower Freeman-Tuckey measure for the K_{RF} (434) than for the Gaussian (4311). The same holds true for the RMSE, which is 75 in the case of the K_{RF} and 192 for the Gaussian.

Tables IV and V give the average results corresponding to each image view for RF and IQ data, respectively. The results show that for all views the K_{RF} and the K_{IQ} yield lower values for both RMSE and Freeman-Tuckey measures as compared to the Gaussian. This observation indicates that the K_{RF} and the K_{IQ} better model the RF data from myocardial tissue. Thus, these regions seem to correspond to partially developed speckle, which cannot be

TABLE V
RMSE AND FREEMAN TUCKEY RESULTS FOR IQ TISSUE REGIONS.

	RMSE		Freeman Tuckey measure	
Orientation	K_{IQ}	Circular Gaussian	K_{IQ}	Circular Gaussian
Apical 4 chamber (A4CH)	61	145	350	1749
Apical 2 chamber (A2CH)	49	107	266	1115
Parasternal long axis (PALA)	14	76	114	681
Parasternal short axis (PASA)	70	230	415	3053

properly reflected through a Gaussian distribution. These results are consistent with previous studies showing that the K distribution provides a good fit to the statistics of the envelope-detected signal from myocardial tissue [14].

VI. Conclusions

In this paper, we have proposed to model the statistics of the RF signal in the case of partially developed speckle through the so-called K_{RF} and K_{IQ} distributions. We have derived the expressions of the corresponding pdfs and moments for both RF and IQ representations of the signal. From these moments, we also derived the estimators for the two parameters of the distributions.

Numerical simulations showed that these estimators exhibit the same behavior as their envelope counterpart. In particular, the bias and variance of the estimators were found to increase with the shape parameter of the distribution, and the so-called implicit and Blacknell estimators yielded the more consistent estimates.

The ability of the K_{RF} and K_{IQ} distributions in modeling RF signals has been evaluated from echocardiographic images in myocardial regions. The results clearly show the reliability of these distributions in representing RF data corresponding to partially developed speckle.

An interesting application of these results consists in the segmentation of echocardiographic images using statistics-based, deformable models, as suggested in [3] and [4]. Additional research is currently underway to apply the described distribution to the segmentation of echocardiographic images from the RF signal. It is expected that the modeling properties of the proposed distribution will give an improvement of the segmentation algorithm in discriminating myocardium from blood pool.

References

[1] D. Boukerroui, A. Baskurt, J. A. Noble, and O. Basset, "Segmentation of ultrasound images-multiresolution 2D and 3D algorithm based on global and local statistics," *Pattern Recognit. Lett.*, vol. 24, pp. 779–790, 2003.

[2] L. Herlin, D. Bereziat, G. Giraudon, C. Nguyen, and C. Graffigne, "Segmentation of echocardiographic images with Markov fields," in *Proc. Eur. Conf. Comput. Vision*, 1994, pp. 201–206.

[3] A. Sarti, C. Corsi, E. Mazzini, and C. Lamberti, "Maximum likelihood segmentation of ultrasound images with Rayleigh distribution," *IEEE Trans. Ultrason., Ferroelect., Freq. Contr.*, vol. 41, no. 4, pp. 435–440, 2005.

[4] I. Dydenko, F. Jamal, O. Bernard, J. D'hooge, I. E. Magnin, and D. Friboulet, "A level set framework with a shape and motion prior for segmentation and region tracking in echocardiography," *Med. Image Analysis*, vol. 10, no. 2, pp. 162–177, 2006.

[5] V. Dutt and J. F. Greenleaf, "Speckle analysis using signal to noise ratios based on fractional order moments," *Ultrason. Imag.*, vol. 17, no. 4, pp. 251–268, 1995.

[6] G. Georgiou and F. S. Cohen, "Statistical characterization of diffuse scattering in ultrasound images," *IEEE Trans. Ultrason., Ferroelect., Freq. Contr.*, vol. 45, no. 1, pp. 57–64, 1998.

[7] P. M. Shankar, J. M. Reid, H. Ortega, C. W. Piccoli, and B. B. Goldberg, "Use of non-Rayleigh statistics for the identification of tumors in ultrasonic B-scans of the breast," *IEEE Trans. Med. Imag.*, vol. 12, pp. 687–692, 1993.

[8] R. F. Wagner, M. F. Insana, and D. G. Brown, "Statistical properties of radio-frequency and envelope-detected signals with applications to medical ultrasound," *J. Opt. Soc. Amer. A*, vol. 4, pp. 910–922, 1987.

[9] V. Dutt and J. Greenleaf, "Ultrasound echo envelope analysis using homodyned K distribution signal model," *Ultrason. Imag.*, vol. 16, pp. 265–287, 1994.

[10] R. C. Molthen, V. M. Narayanan, P. M. Shankar, J. M. Reid, V. Genis, and L. Vergara-Dominguez, "Ultrasound echo evaluation by K-distribution," in *Proc. IEEE Ultrason. Symp.*, 1993, pp. 957–960.

[11] P. M. Shankar, "A model for ultrasonic scattering from tissues based on the K distribution," *Phys. Med. Biol.*, vol. 40, pp. 1633–1649, 1995.

[12] E. Jakeman and P. N. Pusey, "A model for non-Rayleigh sea echo," *IEEE Trans. Antennas Propagat.*, vol. 24, no. 6, pp. 806–814, 1976.

[13] E. Jakeman, "On the statistics of K-distributed noise," *J. Phys. A.*, vol. 13, pp. 31–48, 1980.

[14] L. Clifford, P. Fitzgerald, and D. James, "Non-Rayleigh first-order statistics of ultrasonic backscatter from normal myocardium," *Ultrasound Med. Biol.*, vol. 19, no. 6, pp. 487–495, 1993.

[15] A. C. Frery, H.-J. Muller, C. C. F. Yanasse, and S. J. S. Sant'Anna, "A model for extremely heterogeneous clutter," *IEEE Trans. Geosci. Remote Sensing*, vol. 35, no. 3, pp. 648–659, 1997.

[16] D. D. Blacknell, "Comparison of parameter estimators for K-distribution," *IEE Proc. Radar, Sonar, Navig.*, vol. 141, no. 1, pp. 45–52, 1994.

[17] D. D. Blacknell and R. J. A. Tough, "Parameter estimation for the K-distribution based on $[z \log(z)]$," *IEE Proc. Radar, Sonar, Navig.*, vol. 146, no. 6, pp. 309–312, 2001.

[18] D. R. Iskander and A. M. Zoubir, "Estimating the parameters of K distribution using higher order and fractional moments," *IEEE Trans. Aerosp. Electron. Syst.*, vol. 35, pp. 1453–1457, 1999.

[19] D. R. Iskander, A. M. Zoubir, and B. Boashash, "A method for estimating the parameters of the K distribution," *IEEE Trans. Signal Processing*, vol. 47, no. 4, pp. 1147–1151, 1999.

[20] I. R. Joughin, D. B. Percival, and D. P. Winebrenner, "Maximum likelihood estimation of K distributed parameters for SAR data," *IEEE Trans. Geosci. Remote Sensing*, vol. 31, pp. 989–999, 1993.

[21] R. S. Raghavan, "A method for estimating parameters of K-distributed clutter," *IEEE Trans. Aerosp. Electron. Syst.*, vol. 27, no. 2, pp. 238–246, 1991.

[22] P. Lombardo and C. J. Oliver, "Estimation of texture parameters in K-distributed clutter," *IEE Proc. Radar, Sonar, Navig.*, vol. 141, no. 4, pp. 196–204, 1994.

[23] A. Consortini and F. Rigal, "Fractional moments and their usefulness in atmospheric laser scintillation," *Pure Applied Opt.*, vol. 7, pp. 1013–1032, 1998.

[24] D. S. Moore, "Tests of the chi-squared type," in *Goodness-of-Fit Techniques*. R. B. D'Agostino and M. A. Stephens, Eds. New York: Marcel Dekker, 1986, pp. 63–95.

[25] R. D'Agostino and R. Stephens, *Goodness-of-Fit Techniques*. New York: Marcel Dekker, 1986.